

000  
001  
002  
003  
004  
005  
006  
007  
008  
009  
010  
011  
012  
013  
014  
015  
016  
017  
018  
019  
020  
021  
022  
023  
024  
025  
026  
027  
028  
029  
030  
031  
032  
033  
034  
035  
036  
037  
038  
039054  
055  
056  
057  
058  
059  
060  
061  
062  
063  
064  
065  
066  
067  
068  
069  
070  
071  
072  
073  
074  
075  
076  
077  
078  
079  
080  
081  
082  
083  
084  
085  
086  
087  
088  
089  
090  
091  
092  
093  
094  
095  
096  
097  
098  
099  
100  
101  
102  
103  
104  
105  
106  
107

# Visual Question Answering with Question Understanding and Reasoning

Anonymous ICCV submission

Paper ID \*\*\*\*

## Abstract

Traditional techniques for visual question answering (VQA) are mostly end-to-end neural network based, which often perform poorly (e.g. inefficiency and low accuracy) due to lack of question understanding and necessary reasoning. To overcome the weaknesses, we propose a comprehensive approach with following key features. (1) It represents inputs, i.e. image  $Img$  and question  $Q_{nl}$  as entity-attribute graph and query graph, respectively, and employs graph matching to find answers; (2) it leverages reinforcement learning based model to identify correct query graph, and a set of policies that are used to guide visual tasks, based on  $Q_{nl}$ ; and (3) it trains a classifier and reasons missing values that are crucial for question answering with the classifier. With these features, our approach can not only conduct visual tasks more efficiently, but also answer questions with higher accuracy; better still, our approach also works in an end-to-end manner, owing to seamless integration of our techniques. To evaluate the performance of our approach, we conduct empirical studies on our VQA data set (Soccer-VQA) and Visual-Genome data set [1], and show that our approach outperforms the state-of-the-art method in both efficiency and accuracy.

## 1. Introduction

Visual Question Answering (VQA), the problem of automatically and efficiently answering questions about visual content, has attracted a wide range of attention, since it has a variety of applications in e.g. image captioning, surveillance video understanding, visual commentator robot, etc. Though important, the VQA problem brings a rich set of challenges spanning various domains such as computer vision, natural language processing, knowledge representation, and reasoning. In recent years, VQA has achieved significant progress, owing to the development of deep architectures suited for this task and the creation of large VQA datasets to train these models. However, a number of studies [29, 11] also pointed out that despite recent progress, today's neural network based approaches demon-

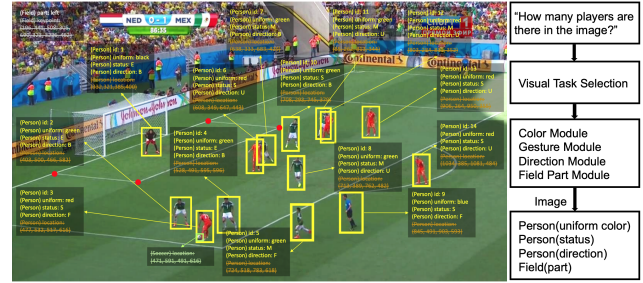


Figure 1: The image is about soccer match, where each person object is associated with attributes: id, uniform color, status (Standing, Moving, Expansion), direction (Backing, Facing, N/A), as well as location, and the soccer object is attributed with location. However, not all informations are necessary in answering one question, visual tasks are selected to achieve acquiring relevant information.

strate a few weaknesses, which greatly hinders its further development. First of all, existing techniques train deep neural networks to predict answers, where image-question pairs are jointly embedded as training data, following this way, the correlation between the question and the image is ignored, which may lead to difficulty in balancing accuracy and efficiency. Secondly, deep neural networks works as “black boxes”, it is very hard to identify the causal relations between network design and system performance, not to mention ensuring acceptable performance. Lastly, due to lack of reasoning capability, existing techniques show poor performance when answering real-life questions, that are often open-ended and require necessary reasoning.

To address the issues mentioned above, a method, that finds answers based on the understanding of the questions and necessary reasoning, is required.

**Example 1:** Figure 1 depicts an image about a soccer match, where each object is associated with a set of attributes. A typical question may ask “How many players are there in the image?”. Though simple, it is a challenging task to efficiently answer the query, since (1) traditionally, it often takes time to extract as much information as possible from the given image, and then answer the questions; while, only question related objects are needed; (2) infor-

108 mation extracted from image alone is often insufficient to  
109 answer questions, hence missing values that are crucial for  
110 question answering should be inferred by certain reasoning  
111 techniques.  
112

113 To tackle the issues, one may (1) model input *i.e.* image  
114 and question, with graph structures that can capture information  
115 from both image and question well, and ease question  
116 understanding and reasoning; (2) follow the work-flow  
117 given on the right hand side of Fig. 1 to identify correct  
118 graph representation of the question, and a set of policies  
119 that are closely related to the question and used to guide  
120 forthcoming visual tasks; and (3) infer values *e.g.* “role”  
121 of person objects (referee, goalkeeper or player) using well  
122 trained classification model. □

123 This example suggests that we address the VQA problem  
124 by modeling inputs as graphs, leveraging techniques to  
125 guide question translation, visual processing, and do reasoning.  
126 While to do this, two critical questions have to be  
127 answered. (1) How to understand questions and carry out  
128 question related visual tasks? (2) How to infer crucial information  
129 to assist question answering?

131 **Contributions.** In contrast to a majority of deep neural  
132 networks based VQA techniques, which not only overlooks  
133 correlation between questions and images, but also lacks of  
134 necessary reasoning, we provide a novel approach that  
135 integrates question understanding and reasoning, for the VQA  
136 problem. The main contributions of the paper are as follow.

137 (1) We model images and questions as graphs, and propose  
138 to answer visual questions with graph matching. This new  
139 representation and answering scheme constitute the  
140 base of our techniques.

141 (2) We introduce a method to guide question translation  
142 and visual processing based on reinforcement learning.  
143 That is, given a question, our method can identify its correct  
144 graph representation, and a set of policies to guide visual  
145 tasks in a more efficient manner.

146 (3) We provide a method to infer missing values to  
147 answer questions. The reasoning task relies on a classifier, that  
148 is generated by offline training with supervised learning.

149 (4) We conduct extensive experimental studies to verify  
150 the performance of our method on both our curated VQA  
151 dataset and a public VQA dataset. We find that X, Y, and Z.

## 153 2. Related Work

154 We categorize related work into following three parts.

155 *Visual query answering.* Current VQA approaches are  
156 mainly based on deep neural works. [32] introduces a  
157 spatial attention mechanism similar to the model for  
158 image captioning. Instead of computing the attention vector  
159 iteratively, [30] obtains a global spatial attention weights

160 vector which is then used to generate a new image embedding.  
161 [31] proposed to model the visual attention as a multivariate  
162 distribution over a grid-structured conditional random field  
163 on image regions, thus multiple regions can be selected at  
164 the same time. This attention mechanism is called structured  
165 multivariate attention in [31]. There has been many other  
166 improvements to the standard deep learning method, *e.g.* [9] utilized  
167 Multimodal Compact Bi-linear (MCB) pooling to efficiently and  
168 expressively combine multimodal features. Another interesting idea is the  
169 implementation of Neural Module Networks [3, 12], which  
170 decomposes queries into their linguistic substructures, and uses  
171 these structures to dynamically instantiate module networks.  
172 [24] proposed to build graph over scene objects and  
173 question words. The visual graph is similar to ours, but the  
174 query graph differs. Note that the method [24] proposed is  
175 still a neural network based method as the structured  
176 representations are fed into a recurrent network to form the final  
177 embedding and the answer is again inferred by a classifier.

178 *Environment Exploration in Visual Field.* Reinforcement  
179 driven information acquisition is not only focusing at  
180 games [27, 26, 14] but also wildly applied in traditional  
181 vision domain. [19] implement reinforcement learning in  
182 visual object detection, by presenting a novel sequential  
183 models which accumulate evidence collected at a small set  
184 of image locations to detect visual objects effectively. [10]  
185 forms the facial detection problem into an adaptive learning  
186 process, by designing an approximate optimal control  
187 framework, based on reinforcement learning to actively  
188 search a visual field. [20] introduced a novel recurrent  
189 neural network model which is capable to extract information  
190 from an image or video by adaptive selection for a sequence  
191 of regions or locations. [33] introduced reinforcement learning  
192 in the task of target-driven visual navigation. Other  
193 works aims to achieving based on algorithms [15, 2].

194 In visual and language domain, relevant work like [23]  
195 achieves image captioning with Embedding Reward. Reinforcement  
196 learning preserves ability to effectively select  
197 preferred actions, which benefits the system decomposing  
198 the problem into a few sub-tasks.

199 *Graph-based visual understanding.* [25] proposes a frame-  
200 work to understand events and answer user queries, where  
201 underlying knowledge is represented by a spatial-temporal-  
202 causal And-Or graph (S/T/C-AOG).

## 203 3. Overview of the Approach

204 We start from representations of images and questions,  
205 followed by the overview of our approach.

### 206 3.1. Representation of Images and Questions

207 We use the same representations as [29]. To make the  
208 paper self-contained, we cite them as follows (rephrased).

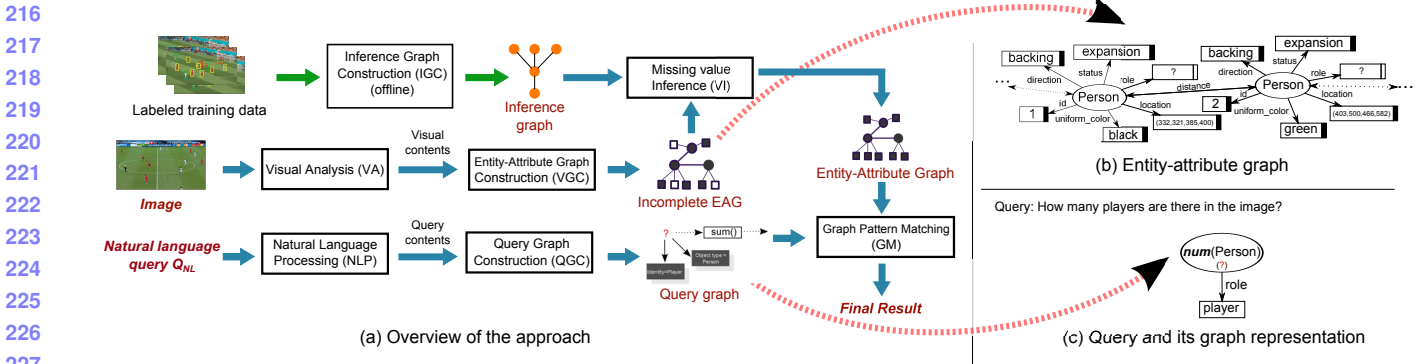


Figure 2: Overview of our approach, and graph-based representation of images and questions

**Entity-Attribute Graphs.** Entities are typically defined as objects or concepts that exist in the real world. An entity often carries attributes, that describe features of the entity.

Assume a set  $\mathcal{E}$  of entities, a set  $\mathcal{D}$  of values, a set  $\mathcal{P}$  of predicates indicating attributes of entities and a set  $\Theta$  of types. Each entity  $e$  in  $\mathcal{E}$  has a *unique ID* and a *type* in  $\Theta$ .

An *entity-attribute* graph, denoted as EAG, is a set of triples  $t = (s, p, o)$ , where *subject*  $s$  is an entity in  $\mathcal{E}$ ,  $p$  is a *predicate* in  $\mathcal{P}$ , and *object*  $o$  is either an entity in  $\mathcal{E}$  or a value  $d$  in  $\mathcal{D}$ . It can be represented as a directed edge-labeled graph  $G_{EA} = (V, E)$ , such that (a)  $V$  is the set of nodes consisting of  $s$  and  $o$  for each triple  $t = (s, p, o)$ ; and (b) there is an edge in  $E$  from  $s$  to  $o$  labeled by  $p$  for each triple  $t = (s, p, o)$ .

An image can be represented as an EAG with detected objects along with their detected attributes, and relationships among objects. This can be achieved via a few visual tasks. While EAG generated directly after image processing is often incomplete, *i.e.* it may miss some crucial information to answer queries. We hence refer to *entity-attribute graphs* with incomplete information as *incomplete entity-attribute graphs*, and associate nodes with white rectangles, to indicate the missing value of an entity or attribute in EAG. Figure 1(b) is an *incomplete entity-attribute graph*, in which square nodes representing person roles are associated with white rectangle.

**Query Graphs.** A query graph  $Q(u_o)$  is a set of triples  $(s_Q, p_Q, o_Q)$ , where  $s_Q$  is either a variable  $z$  or a function  $f(z)$  taking  $z$  as parameter,  $o_Q$  is one of a value  $d$  or  $z$  or  $f(z)$ , and  $p_Q$  is a predicate in  $\mathcal{P}$ . Here function  $f(z)$  is defined by users, and variable  $z$  has one of three forms: (a) *entity variable*  $y$ , to map to an entity, (b) *value variable*  $y^*$ , to map to a value, and (c) *wildcard*  $_y$ , to map to an entity. Here  $s_Q$  can be either  $y$  or  $_y$ , while  $o_Q$  can be  $y$ ,  $y^*$  or  $_y$ . Entity variables and wildcard carry a *type*, denoting the type of entities they represent.

A query graph can also be represented as a graph such that two variables are represented as the same node if they

have the same name of  $y$ ,  $y^*$  or  $_y$ ; similarly for functions  $f(z)$  and values  $d$ . We assume *w.l.o.g.* that  $Q(x)$  is connected, *i.e.* there exists an undirected path between  $u_o$  and each node in  $Q(u_o)$ . In particular,  $u_o$  is a designated node in  $Q(u_o)$ , denoting the query focus and labeled by “?”. Take Fig. 2(c) as example. It depicts a query graph that is generated from query “*How many players are there in the image?*”. Note that the “query focus”  $u_o$  carries a function  $num()$  that calculates the total number of *person* entities with *role* “player”.

### 3.2. Approach Overview

Figure 2(a) presents the overview of our approach. In a nutshell, our approach takes an image and a natural language question  $Q_{NL}$  as input, and answers questions with seven modules as following. (1) Upon receiving a question  $Q_{NL}$ , module QVS identifies a set of visual tasks that are query-oriented and category of the query graph that corresponds to the input question, and passes tasks and category to modules VTP and QGC, respectively. (2) Guided by the list of tasks, module VTP conducts visual tasks over the input image, and returns identified objects along with their attributes to module VGC. (3) Module VGC constructs an entity-attribute graph  $G_{EA}$ , by using identified objects and their attributes. Note that  $G_{EA}$  may be incomplete and hence unable to answer questions. (4) When  $G_{EA}$  is incomplete, module VI infers missing value with a classifier  $G_I$ , denoted as *inference graph*, and produces an updated EAG for question answering. (5) Module QGC takes category of the query graph as input, and generates a query graph  $Q(u_o)$ . (6) After  $Q(u_o)$  and  $G_{EA}$  are generated, module GM is invoked for matching computation, and returns final result. (7) In contrast to online computation that are processed by above modules, the module IGC constructs *inference graphs* using labeled training data, offline.

As some modules employ existing techniques, to emphasize our novelty, we will elaborate modules VA and VGC in Section ??, modules IGC and VI in Section ??, and module GM in Section ?? with more details.

324

## 4. Question Oriented Visual Tasks

325  
326  
327

In this section, we introduce how we do visual tasks that are in connection with questions.

328  
329

### 4.1. Visual Processing

330  
331  
332  
333  
334  
335  
336  
337  
338

In our approach, we build a structure which selects sub-tasks to form a policy which is based on queries. For instance, with the input *which is the defending team?*, the system first predicts the corresponding visual action sequence, which are *Human Module*, *Gesture Module*, *Direction Module*, *Soccer Module*, *Color Blob Module*, *Field Part Module* and *Graph Indicator*. Guided by such sequence, the image features are then extracted by operating relevant vision tasks. An overview is shown in Figure 3.

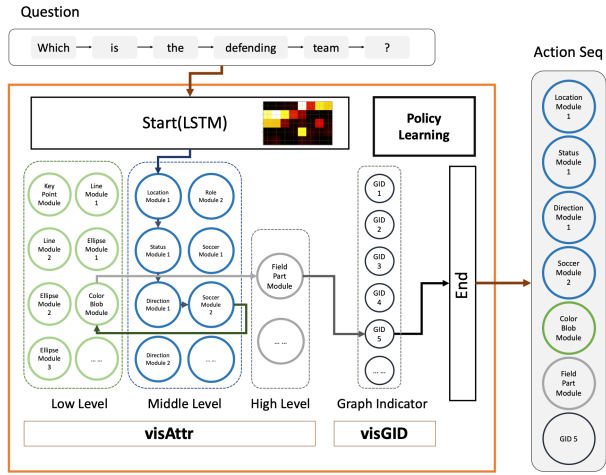


Figure 3: Visual Processing Strategy

355

356

357  
358  
359

#### 4.1.1 Multi-layer LSTM with Attention

360  
361  
362  
363  
364  
365  
366  
367  
368  
369  
370  
371

The task here is to predict the most suitable action modules sequence  $a$  by given questions  $Q$  and preference  $pre$ . We form the problem of seeking effective answering strategy of question  $Q$  and preference  $pre$  as a sequence-to-sequence learning problem with attention mechanism. Inspired by [5], we input word feature of questions  $w_i^q$ ,  $i \in \|Q\|$  into a LSTM network which is regarded as an encoder and output  $h_i$  as the hidden state for  $i$ th word in the question. By adding soft attention, the context vector  $c_i$  is calculated by the following equations.

372  
373  
374  
375  
376  
377

$$c_i = \sum_{j=1}^{\|Q\|} a_{ij} h_j \quad (1)$$

$$a_{ij} = \frac{\exp(e_{ij})}{\sum_{k=1}^{\|Q\|} \exp(e_{ik})} \quad (2)$$

$$e_{ij} = a(s_{j-1}, h_i) \quad (3)$$

378

379

380

381

382

383

384

385

386

387

388

389

390

391

392

393

394

395

396

397

398

399

400

401

402

403

404

405

406

407

408

409

410

411

412

413

414

415

416

417

418

419

420

421

422

423

424

425

426

427

428

429

430

431

where  $h_i$  and  $s_j$  are hidden states of encoder and decoder stage, respectively. Here  $a_{ij}$  is the attention weights, with higher  $a_{ij}$  in  $(i, j)$  pair, the more attention will pay in this correlation, thus the  $j$ th output action  $a_i$  module will be more influenced by the  $i$ th input word  $w_i^q$  in question. The decode part is similar as traditional recurrent neural networks (RNN). The following steps demonstrates decoding to get the joint distribution of action module sequence  $A = [a_1, \dots, a_t]$ .

$$p(A|Q) = \prod_{t \in \|A\|} p(a_t | \{a_1, \dots, a_t\}, c_i, Q) \quad (4)$$

$$p(a_t | \{a_1, \dots, a_t\}, c_i, Q) = g(a_{t-1}, s_t, c_i, Q) \quad (5)$$

$$s_t = f(s_{t-1}, a_{t-1}, c_i) \quad (6)$$

where  $g(\cdot)$  is a nonlinear function which outputs the probability of action module  $a_t$ . The probability distribution  $p(A|Q)$  is used to predict a maximum probability action module sequence by beam search during testing time.

Guided by this action sequence  $[a_1, a_2, a_3, \dots, a_n]$ , actions are selected from the following visual task pool, and comes into next session, visual task selection (VTS).

#### 4.1.2 Visual Task Selection

VTS is guided by the question feature, selecting target visual tasks from the visual task pool by Monte Carlo learning. The task pool is demonstrated in Table 1.

	Level	Sub-task	Descriptions
visAttr	Low	Keypoint Module	To get detailed information of the soccer field $F_{keypoint}$ .
		Line Module	
		Ellipse Module	
	Middle	Color Blob Module	To detect blobs of different colors among a region ( whole soccer field or a small bounding box).
		Location Module	To detect the location of the person $P_{location}$ .
	High	Status Module	To get the person's gesture $P_{status}$ (standing, moving, expansion).
		Direction Module	To get whether a person is facing the goal or not $P_{direction}$ .
		Uniform Module	To get the uniform color of the person $P_{uniform}$ .
visGID	High	Soccer Module	To detect the location of the soccer $S_{location}$ .
		Field Part Module	To detect which part of the soccer field is there in the image $F_{part}$ .
visGID	Graph ID Indicator	To indicate which type of graph will be used in the following process.	

Table 1: Visual Task Pool

The pool is constructed by two parts, the first one is  $visAttr$  which aims to discover the attribute of people, soccer, field and scene [29], while the other one  $visGID$  is an indicator showing the current question belongs to which graph type. There are three levels of  $visAttr$ : low, middle and high, which represents different degree of the vision tasks.



Figure 4: Person status.

For each vision task, the approach is not fixed, one task can be achieved by different methods with variance in time and accuracy. For instance, object detection based methods, like Faster R-CNN [22], R-FCN [7], SSD [17] or skeleton keypoints detection based method like [6] and [28] can be implemented as a set of status module methods, because all of them is able to localize and distinguish people who are moving, standing or with an expansion gesture (Figure 4). Thus, the system is not only able to determine whether resembles a vision task module into action module sequence  $[a_1, a_2, a_3, \dots, a_n]$ , it can also select one specific approach under a vision task module, based on question and preference. For the preference, it is clarified in the next section.

#### 4.1.3 Time and Accuracy Term

To better balance the accuracy and inference time for a given application, we proposed time and accuracy terms in loss function during training process.

$$L_{\tau\alpha}(\theta) = \ell(\theta, A|I, Q) + \gamma \sum_{i \in \|A\|} \alpha(a_i) + (1 - \gamma) \sum_{i \in \|A\|} \tau(a_i) \quad (7)$$

where  $\tau(\cdot)$  and  $\alpha(\cdot)$  represent the pre-tested inference time and inference accuracy, action module sequence  $A$  samples from joint distribution  $p(A|Q)$ , and here  $\ell(\cdot)$  is the softmax loss over the predict score. For the preference term  $\gamma$ , it ranges from 0 to 1, which represents the preference over time and accuracy.

#### 4.1.4 Monte Carlo Methods

The task now becomes a policy learning problem. Given a question and preference, output a policy containing a sequence of actions  $[a_1, a_2, a_3, \dots, a_n]$ . There is no ground truth for each steps, but only a final reward indicates that whether the prediction result is correct based on current policy. We involve the concept of Monte Carlo Methods to learn the policy which guides the vision tasks, and such policy network requires an extra reward value in loss.

$$L_{policy}(\theta) = \sum_{i \in \|A\|} \log \pi(a_i|Q, \theta) \ell(Q, A) \quad (8)$$

where  $a_i$  is the action will take, based on current status.  $\pi(\cdot)$  is the policy function that maps status to actions,

here, the policy is the probability of outputing next action module  $a_i$  based on current status. And  $\ell(\cdot)$  here is the softmax loss based on the whole action module sequence  $[a_1, a_2, a_3, \dots, a_n]$ . Since all actions are discrete, which leads to non-differentiable, and back-propagation cannot be used. Policy gradient [16] is used here during training. The object function now becomes the combination of policy gradient loss  $L_{policy}(\theta)$  with the time-accuracy-balanced loss  $L_{\tau\alpha}$ , and optimize it by backpropagation for  $L_{\tau\alpha}$ , while policy gradient for  $L_{policy}(\theta)$ .

### 4.2. Construction of EAG

After objects that are related to questions are identified, we construct a graph structure, denoted as EAG, along the same line as [29].

**Example 2:** ADD AN EXAMPLE TO ILLUSTRATE PROGRESS IF NECESSARY!  $\square$

## 5. Reasoning

According to our observation, an *incomplete* EAG isn't well satisfying of answering the question because of the insufficient attributes. To infer the hidden attributes, an inference graph is constructed accordingly. we briefly introduce the construction below.

### 5.1. Construction of Inference Graph

To take advantage of the prior information and increase the generalization ability of the proposed model, our inference graph is constructed using Bayesian network. Mathematically, Bayesian network [8] can be described by a pair  $\mathcal{B} = < \mathcal{G}, \Theta_{\mathcal{G}} >$ . Here, the notation  $\mathcal{G}$  is a directed acyclic graph, of which the  $i$ -th vertex corresponds to a random variable  $X_i$ , and the edge between two connected vertexes indicates the dependency. Additionally, the second item  $\Theta_{\mathcal{G}}$  is a set of parameters used to quantify the dependencies in  $\mathcal{G}$ . Denoted by  $\text{Pa}(X_i)$  the attributes of the parents of  $X_i$ , the parameter of  $X_i$  is represented by  $\theta_{X_i|\text{Pa}(X_i)} = P_{\mathcal{B}}(X_i|\text{Pa}(X_i))$ . With the notations above, the joint probability distribution of Bayesian network is given by:

$$P_{\mathcal{B}}(X_1, \dots, X_n) = \prod_{i=1}^n P_{\mathcal{B}}(X_i|\text{Pa}(X_i)) = \prod_{i=1}^n \theta_{X_i|\text{Pa}(X_i)} \quad (9)$$

In our inference graph, the role of Bayesian network is to predict the object class when given the attributes  $\{X_i\}_{i=1}^n$  as input. In the sense of probability, the object class is also a variable [13]. Defined by  $X_0 = Y$  the class variable, the network now has one extra vertex  $X_0$ . In order to infer the class attribute, and according to the Bayesian rule, our problem becomes:

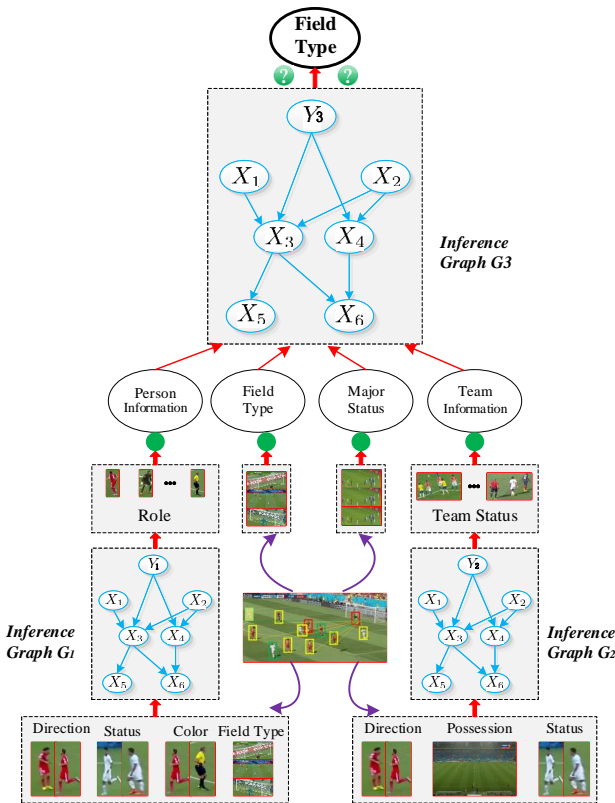


Figure 5: Schematic diagram of inference graph.

$$P_{\mathcal{B}}(Y|X) = \frac{P_{\mathcal{B}}(Y)P_{\mathcal{B}}(X|Y)}{P_{\mathcal{B}}(X)} \quad (10)$$

$$= \frac{\theta_{Y|\text{Pa}(X_0)} \prod_{i=1}^n \theta_{X_i|Y, \text{Pa}(X_i)}}{\sum_{y' \in \mathcal{Y}} \theta_{y'|\text{Pa}(X_0)} \prod_{i=1}^n \theta_{X_i|y', \text{Pa}(X_i)}}$$

where  $\mathcal{Y}$  is the set of classes.

## 5.2. Learning the Structure of Inference Graph

In the context of Naïve Bayes, the structure of  $P_{\mathcal{B}}(Y|X)$  is simplified by taking the class variable as the root, and all attributes are conditionally independent when taking the class as a condition [21]. As a consequence, the attribute class can be explicitly inferred by:

$$P_{\mathcal{B}}(Y|X) = c \cdot \theta_Y \prod_{i=1}^n \theta_{X_i|Y} \quad (11)$$

where  $c$  is a scale factor that makes the calculation being a distribution:  $c = \sum_{y' \in \mathcal{Y}} \theta_{y'} \prod_{i=1}^n \theta_{X_i|y'}$ .

One can observe from Eq.(11) that Naïve Bayes simplifies the complexity of Bayesian network. As can be validated by the experimental results, this simple model works excellently to our problem.

In the area of VQA, some simple questions may need the implicit attributes to assist the answering system to

find out the final answer. As a closely related example, a typical problem may be “how many players are there in the image?”. In this case, not only all the *person* objects are needed to be identified, but also the hidden attribute: the role of each person.

**Figure 5** summarizes the processes of our inference graph, where three graphs are constructed according to the tasks involved. First, the role of a candidate is inferred from  $G_1$ , in which four different kinds of features are extracted from the scene image. Then, the team status is inferred through the second inference graph  $G_2$ , but with different features as input. Next, we use the inferred information, along with the other information can be directly detected from the scene image, to infer the information of the whole scene. The scene information is then fed into the incomplete EAG so that a complete EAG can be obtained.

## 6. Experimental Studies

In this section, we conduct two sets of experiments to evaluate (1) the performance of our visual processing module, (2) the accuracy of our inference module, and (3) the overall performance of our approach.

### Experimental Setting.

**DataSet.** We used two data sets: (1) Soccer dataset that we annotated; and (2) Visual Genome dataset from <http://visualgenome.org>. We extracted images with subjects of golf and tennis. We split Soccer data into two parts: *I* (one third) and *II* (two thirds), and used *II* as training data, and *I* as testing data.

**Questions.** We used two sets of questions: (1) the set of questions given in **Table 2** for Soccer dataset; and (2) another set of questions for Visual Genome dataset, and the question types listed in **Table 2**.

(We enlarge the training question scale from 7 into 28, so learning correlation between question and answer does not work at this time. For question details, please refer [questionset.txt.rtf](#).)

### 6.1. Generalization Ability of Model

To test the generalization of our method, we enlarge the training set by more various question with same meaning. For instance, the original question of  $Q_{nl5}$  is “Who is the defending team?”. We add three more similar questions asking Who is attacking team?, “What is the uniform color of the defending team?” and “What is the uniform color of the attacking team?”. Unlike state-of-art methods answering questions in [29], adding generalization and variation in questions would not dramatically change the performance. It is because the structure is not fixed, and all the visual task selection is query oriented. For [12], even though the network is not fixed, the answering part is based on neural

648	<b>Id</b>	<b>Question</b>	<b>Difficulty</b>
649	$Q_{nl_1}$	Who is holding the soccer?	Easy
650	$Q_{nl_2}$	What is the uniform color of the referee?	Easy
651	$Q_{nl_3}$	Is there any referee in the image?	Easy
652	$Q_{nl_4}$	Which team does the goalkeeper belong to?	Medium
653	$Q_{nl_5}$	Who is the defending team?	Medium
654	$Q_{nl_6}$	Which part of the field are the players being now?	Hard
655	$Q_{nl_7}$	How many players are there in the image?	Hard
656	$Q_{nl_8}$	Is this image about corner kick? <i>(If not, just list the correct one.)</i>	??
657	$Q_{nl_9}$	Is this image about free kick? <i>(If not, just list the correct one.)</i>	??
658	$Q_{nl_{10}}$	Is this image about kick off? <i>(If not, just list the correct one.)</i>	??
659	$Q_{nl_{11}}$	Is this image about penalty kick? <i>(If not, just list the correct one.)</i>	??

Table 2: A set of questions

network, and essentially it also learns the statically correlation, which leads to the weakness in logical reasoning. The result is shown in Table 3.

Various Training Questions		Original Training Questions	
Methods	Acc (%)	Methods	Acc (%)
CNN+LSTM	28.14	CNN+LSTM	46.40
HieCoAttenVQA	31.92	HieCoAttenVQA	49.11
Learning2Reason	38.00	Learning2Reason	51.08
Ours	64.02	Ours	66.75

Table 3: Generalization of our method

## 6.2. Performance of Visual Task Selecting Policy

To test the validity of reinforcement learning of selecting visual task modules, we test the inference time over accuracy with the state-of-art [4] [18] which is shown in ??.

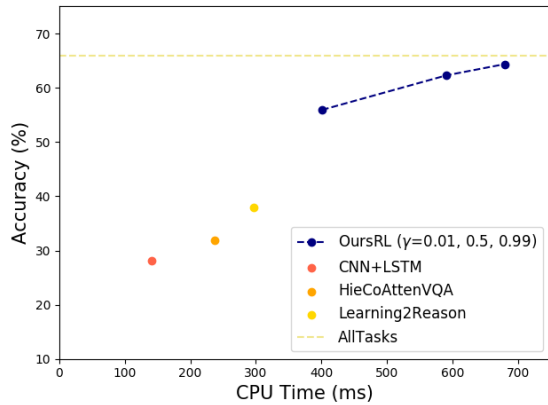


Figure 6: Inference time and accuracy.

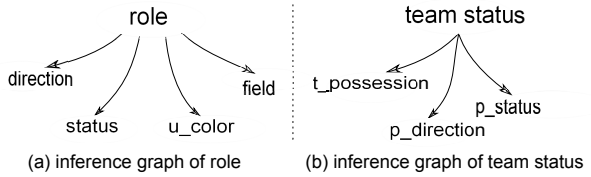


Figure 7: Inference graphs

## 6.3. Effectiveness of Inference

In VQA task, we aim to achieve great performance with short responding time. “CPU Time” evaluates the time cost from features extraction to question answering. All the computation work is implemented on CPU.

In terms of system accuracy, we follow the F-measure. Define that  $\#true\_value\_inferred$  is the total number of instances whose attribute  $A$  is “ $v$ ” and is inferred correctly as “ $v$ ”,  $\#true\_value\_instance$  is the number of all the instances with attribute  $A$  of value “ $v$ ”, and  $\#inferred\_instances$  indicates the total number of instances whose attribute  $A$  is inferred as “ $v$ ”. The inference accuracy can be defined as below.

$$Acc(A = "v") = \frac{2 \cdot (recall(A = "v")) \cdot precision(A = "v"))}{recall(A = "v") + precision(A = "v"))} \quad (12)$$

where:

$$\begin{aligned} recall(A = "v") &= \frac{\#true\_value\_inferred}{\#true\_value\_instance} \\ precision(A = "v") &= \frac{\#true\_value\_inferred}{\#inferred\_instance} \end{aligned}$$

We compare our approach to the state-of-the-art systems, i.e. CNN+LSTM[??], HieCoAttenVQA[??], and Learning2Reason[??].

	Time (ms)	Acc (%)
CNN+LSTM	141	28.14
HieCoAttenVQA	237	31.92
Learning2Reason	297	38.00
Ours (without RL)	N/A	65.85
Ours ( $\gamma = 0.01$ )	401	55.92
Ours ( $\gamma = 0.50$ )	591	62.29
Ours ( $\gamma = 0.99$ )	680	64.02

Table 4: Inference time and accuracy comparison.

**Table 4** lists the time cost and accuracy results among different approaches. For CNN+LSTM, HieCoAttenVQA, and Learning2Reason, their systems work quite efficient with responding time less than 300ms. But the accuracies of these three approaches are lower than 40%, which is unacceptable. Whereas, the system similar to [29] outperforms all other methods and reaches 65.86% accuracy, but it costs

756 much more time. Our approach is able to keep balance  
 757 between effectiveness and efficiency. For effectiveness,  
 758 our approach achieves 64.02% accuracy, which is 35.88%,  
 759 32.10% and 26.02% higher than results of CNN+LSTM,  
 760 HieCoAttenVQA, and Learning2Reason, respectively. For  
 761 efficiency, our approach can reduce the inference time by  
 762 choosing a small value of  $\gamma$ .  
 763

#### Accuracy of Role

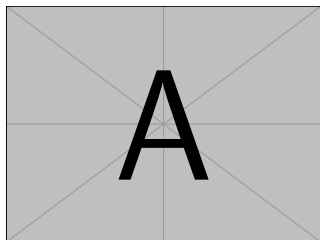
764 Based on questions and image characteristics, four  
 765 variables including *direction*, *status*, *field*, and  
 766 *unique\_color* (abbr. *u\_color*) are adopted to calculate  
 767 conditional probabilities. The inference graph is shown  
 768 in [Figure 7](#) and the inference results are given in [Table 5](#).  
 769 It is easy to find that the inference accuracy for role player  
 770 reaches 99%, which is highest among all roles. And the  
 771 accuracies for different roles are all above 85%.  
 772

Role	Precision	Recall	Acc
Goalkeeper	94.4	85.5	89.8
Referee	87.4	82.8	85.0
Player	98.8	99.3	99.0

773 Table 5: Inference accuracy of role (%).  
 774  
 775  
 776  
 777

778 Using the conditional probabilities, *VI* ([???](#)) infers role  
 779 of each person object. The inference accuracy is shown in  
 780 [Table 5](#). It is easy to find that the inference accuracy for role  
 781 player reaches 99%, which is highest among all roles. And the  
 782 accuracies for different roles are all above 85%.  
 783

#### Accuracy of Team Status



784 Figure 8: Attributes of team inference graph.  
 785  
 786

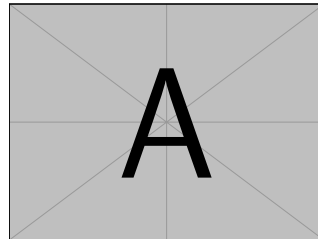
Team Status	Precision	Recall	Acc
Defending	89.8	74.2	81.3
Attacking	79.1	92.1	85.1

804 Table 6: Inference accuracy of team status (%).  
 805  
 806

807 [Table 6](#) gives the performance of our approach for infer-  
 808 ring team status. In general, inference results of defending  
 809 and attacking are both above 80% accuracy. To be specific,

810 the accuracy for inferring if a team is attacking achieves  
 811 85.1%, which is higher than the inference accuracy for de-  
 812 fending status detection by 3.8%.  
 813

#### Accuracy of Field Scene



814 Figure 9: Attributes of scene inference graph.  
 815  
 816  
 817

818 Field Scene includes four different scenes, *i.e.* corner  
 819 kick, free kick, penalty kick and kick-off. Practically, cor-  
 820 ner kick scene always happens as a single player kick the  
 821 ball within a one-yard radius of the corner flag and most of  
 822 players gather in the penalty field. Free kick happens out-  
 823 side the penalty area and defensive wall exists mostly. It  
 824 is much typical for the penalty kick scene because most of  
 825 players are out of penalty area except kick player and goal-  
 826 keeper with football in the penalty spot. As for kick-off  
 827 scene, the ball is played in the center spot with all mem-  
 828 bers of the opposing team at least 10 yards from the ball.  
 829 Based on these observations, we design an inference graph  
 830 in [Figure 9](#).  
 831

832 Inference results are indicated in [Table 7](#) based on infer-  
 833 ence graph in [Figure 9](#). As is shown, the inference accu-  
 834 racy of corner kick, free kick, kick-off and penalty kick are  
 835 59.57%, 63.16%, 85.94% and 60.00%, respectively. It is  
 836 obvious that the scene of kick off reaches the highest accu-  
 837 racy among all.  
 838

Field Type	Precision	Recall	Acc
Corner-kick	59.57	68.29	63.64
Free-kick	63.16	58.54	60.76
Kick-off	85.94	82.09	83.97
Penalty-kick	60.00	60.00	60.00
Ave.	71.28	70.73	70.89

841 Table 7: Inference accuracy of field scene with the proposed  
 842 approach (%).  
 843  
 844  
 845  
 846  
 847

848 In addition, we compare our approach with NuSVC,  
 849 MLP, and AdaBoost in [Table 8](#). The results show that the  
 850 average accuracy of our approach is higher than that of  
 851 NuSVC and AdaBoost by 4.49% and 5.97% respectively,  
 852 and slightly better than that of MLP.  
 853

	Precision	Recall	Acc
NuSVC	68.30	65.85	66.40
MLP	70.80	<b>70.73</b>	70.32
AdaBoost	65.50	65.24	64.92
Ours	<b>71.28</b>	<b>70.73</b>	<b>70.89</b>

Table 8: Average accuracy comparison of field scene (%).

## 6.4. Overall Performance

We compare our proposed method with the following state-of-art methods: LSTM+CNN, HieCoAttenVQA, and Learn2Reason. The results are listed in Table 9. The average accuracy using our approach is higher than that of CNN+LSTM, HieCoAttenVQA and Learn2Reason by 20.35%, 17.64% and 15.67%, respectively.

	CNN+LSTM	HieCoAtten	Learn2Reason	Ours
$Q_{nl1}$	44.23	43.62	31.12	<b>64.86</b>
$Q_{nl2}$	71.31	<b>77.66</b>	9.4	63.74
$Q_{nl3}$	74.58	<b>83.78</b>	83.21	70.00
$Q_{nl4}$	40.48	39.29	51.92	<b>62.14</b>
$Q_{nl5}$	49.19	49.90	30.78	<b>62.58</b>
$Q_{nl6}$	20.56	18.70	30.0	<b>93.33</b>
$Q_{nl7}$	11.08	12.63	36.69	<b>50.60</b>
Avg.	46.40	49.11	51.08	<b>66.75</b>

Table 9: Accuracy comparison per question and average for Soccer Dataset (%).

	CNN+LSTM	HieCoAtten	Learn2Reason	Ours
$Q_{t1}$	63.72	64.83	<b>67.12</b>	65.59
$Q_{t2}$	22.87	24.52	25.04	<b>82.87</b>
$Q_{t3}$	36.96	37.89	<b>40.12</b>	34.16
Avg.	50.48	51.67	53.71	<b>63.41</b>

Table 10: Accuracy comparison per question type and average for Visual Genome Dataset (%).

To evaluate the generalization of the proposed scheme, we measure its accuracy on Visual Genome Dataset. Results in Table 10 show that our approach can handle different types of questions, and the overall performance of our approach surpasses CNN+LSTM, HieCoAttenVQA and Learn2Reason by 12.93%, 11.74% and 9.7%, respectively.

## 7. Conclusion

In this paper, we proposed an innovative and efficient approach to handle the VQA problem. In the proposed

method, the image and question are converted to entity-attribute graph and pattern query, respectively. Then, the reinforcement learning technique is utilized to select the pattern query that is helpful to the visual tasks, in which the missing attributes are inferred by the inference graph constructed from a Bayes network. Last but not the least, the answer is found by graph matching. The generalization of the proposed scheme is significantly improved by introducing the reinforcement learning and inference graph. More importantly, the inference graph here is used in a novel way to make the graph works adaptively. To be specific, the low-level but unknown information is inferred from the known attributes by the inference network, and the high-level but unknown information is finally inferred when the unknown attributes are well inferred. The experimental results encouragingly demonstrate that the proposed scheme corroborates the efficiency and high accuracy when compared with other state-of-the-art baseline methods on two data sets.

The problem of VQA has been widely studied using the graph manner but with slight satisfaction. The reason may concern the integration of external data with complex reasoning tasks, the improvement of inference scheme, and the interactive strategy.

## References

- [1] Visual genome dataset. <http://visualgenome.org>. 1
- [2] F. Abtahi and I. R. Fasel. Deep belief nets as function approximators for reinforcement learning. In *Lifelong Learning, Papers from the 2011 AAAI Workshop, San Francisco, California, USA, August 7, 2011*, 2011. 2
- [3] J. Andreas, M. Rohrbach, T. Darrell, and D. Klein. Neural module networks. *2016 IEEE Conference on Computer Vision and Pattern Recognition (CVPR)*, Jun 2016. 2
- [4] S. Antol, A. Agrawal, J. Lu, M. Mitchell, D. Batra, C. L. Zitnick, and D. Parikh. VQA: Visual Question Answering. In *International Conference on Computer Vision (ICCV)*, 2015. 7
- [5] D. Bahdanau, K. Cho, and Y. Bengio. Neural machine translation by jointly learning to align and translate. May 2016. 4
- [6] Z. Cao, T. Simon, S.-E. Wei, and Y. Sheikh. Realtime multi-person 2d pose estimation using part affinity fields. In *CVPR*, 2017. 5
- [7] J. Dai, Y. Li, K. He, and J. Sun. R-FCN: object detection via region-based fully convolutional networks. In *Advances in Neural Information Processing Systems 29: Annual Conference on Neural Information Processing Systems 2016, December 5-10, 2016, Barcelona, Spain*, pages 379–387, 2016. 5
- [8] N. Friedman, D. Geiger, and M. Goldszmidt. Bayesian network classifiers. *Machine learning*, 29(2-3):131–163, 1997. 5
- [9] A. Fukui, D. H. Park, D. Yang, A. Rohrbach, T. Darrell, and M. Rohrbach. Multimodal compact bilinear pooling

- 972 for visual question answering and visual grounding. *arXiv preprint arXiv:1606.01847*, 2016. 2
- 973
- 974 [10] B. Goodrich and I. Arel. Reinforcement learning based vi-
- 975 sual attention with application to face detection. In *2012 IEEE Computer Society Conference on Computer Vision and*
- 976 *Pattern Recognition Workshops, Providence, RI, USA, June 16-21, 2012*, pages 19–24, 2012. 2
- 977
- 978 [11] Y. Goyal, T. Khot, D. Summers-Stay, D. Batra, and D. Parikh. Making the v in vqa matter: Elevating the role
- 979 of image understanding in visual question answering. *2017 IEEE Conference on Computer Vision and Pattern Recog-*
- 980 *nition (CVPR)*, Jul 2017. 1
- 981
- 982 [12] R. Hu, J. Andreas, M. Rohrbach, T. Darrell, and K. Saenko. Learning to reason: End-to-end module networks for visual
- 983 question answering. *CoRR, abs/1704.05526*, 3, 2017. 2, 6
- 984
- 985 [13] D. Koller, N. Friedman, and F. Bach. *Probabilistic graphical*
- 986 *models: principles and techniques*. MIT press, 2009. 5
- 987
- 988 [14] M. Lanctot, V. Zambaldi, A. Gruslys, A. Lazaridou, K. Tuyls, J. Perolat, D. Silver, and T. Graepel. A unified
- 989 game-theoretic approach to multiagent reinforcement learning.
- 990 In I. Guyon, U. V. Luxburg, S. Bengio, H. Wallach, R. Fergus, S. Vishwanathan, and R. Garnett, editors, *Ad-*
- 991 *vances in Neural Information Processing Systems 30*, pages 4190–4203. Curran Associates, Inc., 2017. 2
- 992
- 993 [15] S. Lange and M. Riedmiller. Deep auto-encoder neural
- 994 networks in reinforcement learning. In *The 2010 International Joint Conference on Neural Networks (IJCNN)*, pages 1–8,
- 995 July 2010. 2
- 996
- 997 [16] S. Liu, Z. Zhu, N. Ye, S. Guadarrama, and K. Murphy. Improved image captioning via policy gradient optimization of
- 998 spider. In *The IEEE International Conference on Computer*
- 999 *Vision (ICCV)*, Oct 2017. 5
- 1000
- 1001 [17] W. Liu, D. Anguelov, D. Erhan, C. Szegedy, S. E. Reed,
- 1002 C. Fu, and A. C. Berg. SSD: single shot multibox detector.
- 1003 In *Computer Vision - ECCV 2016 - 14th European Con-*
- 1004 *ference, Amsterdam, The Netherlands, October 11-14, 2016, Proceedings, Part I*, pages 21–37, 2016. 5
- 1005
- 1006 [18] J. Lu, J. Yang, D. Batra, and D. Parikh. Hierarchical
- 1007 question-image co-attention for visual question answering,
- 1008 2016. 7
- 1009
- 1010 [19] S. Mathe, A. Pirinen, and C. Sminchisescu. Reinforcement
- 1011 learning for visual object detection. In *2016 IEEE Con-*
- 1012 *ference on Computer Vision and Pattern Recognition, CVPR*
- 1013 *2016, Las Vegas, NV, USA, June 27-30, 2016*, pages 2894–
- 1014 2902, 2016. 2
- 1015
- 1016 [20] V. Mnih, N. Heess, A. Graves, and K. Kavukcuoglu. Recur-
- 1017 rent models of visual attention. In *Advances in Neural Infor-*
- 1018 *mation Processing Systems 27: Annual Conference on Neu-*
- 1019 *ral Information Processing Systems 2014, December 8-13*
- 1020 *2014, Montreal, Quebec, Canada*, pages 2204–2212, 2014.
- 1021 2
- 1022
- 1023 [21] F. Petitjean, W. Buntine, G. I. Webb, and N. Zaidi. Accurate
- 1024 parameter estimation for bayesian network classifiers using
- 1025
- 1026 hierarchical dirichlet processes. *Machine Learning*, 107(8–
- 1027 10):1303–1331, 2018. 6
- 1028
- 1029 [22] S. Ren, K. He, R. Girshick, and J. Sun. Faster r-cnn: Towards
- 1030 real-time object detection with region proposal networks. In *Proceedings of the 28th International Conference on Neural*
- 1031 *Information Processing Systems - Volume 1, NIPS’15*, pages 91–99, Cambridge, MA, USA, 2015. MIT Press. 5
- 1032
- 1033 [23] Z. Ren, X. Wang, N. Zhang, X. Lv, and L. Li. Deep rein-
- 1034 forcement learning-based image captioning with embedding
- 1035 reward. In *2017 IEEE Conference on Computer Vision and*
- 1036 *Pattern Recognition, CVPR 2017, Honolulu, HI, USA, July 21-26, 2017*, pages 1151–1159, 2017. 2
- 1037
- 1038 [24] D. Teney, L. Liu, and A. van den Hengel. Graph-
- 1039 structured representations for visual question answering.
- 1040 *arXiv preprint*, 2017. 2
- 1041
- 1042 [25] K. Tu, M. Meng, M. W. Lee, T. E. Choe, and S. C. Zhu. Joint
- 1043 video and text parsing for understanding events and answer-
- 1044 ing queries. *IEEE MultiMedia*, 21(2):42–70, 2014. 2
- 1045
- 1046 [26] X. Wang and T. Sandholm. Reinforcement learning to play
- 1047 an optimal nash equilibrium in team markov games. In S. Becker, S. Thrun, and K. Obermayer, editors, *Advances*
- 1048 *in Neural Information Processing Systems 15*, pages 1603–
- 1049 1610. MIT Press, 2003. 2
- 1050
- 1051 [27] C.-Y. Wei, Y.-T. Hong, and C.-J. Lu. Online reinforcement
- 1052 learning in stochastic games. In I. Guyon, U. V. Luxburg,
- 1053 S. Bengio, H. Wallach, R. Fergus, S. Vishwanathan, and
- 1054 R. Garnett, editors, *Advances in Neural Information Process-*
- 1055 *ing Systems 30*, pages 4987–4997. Curran Associates, Inc.,
- 1056 2017. 2
- 1057
- 1058 [28] S.-E. Wei, V. Ramakrishna, T. Kanade, and Y. Sheikh. Con-
- 1059 volutional pose machines. In *CVPR*, 2016. 5
- 1060
- 1061 [29] P. Xiong, H. Zhan, X. Wang, B. Sinha, and Y. Wu. Visual
- 1062 query answering by entity-attribute graph matching and rea-
- 1063 soning. In *CVPR*, 2019. 1, 2, 4, 5, 6, 7
- 1064
- 1065 [30] H. Xu and K. Saenko. Ask, attend and answer: Exploring
- 1066 question-guided spatial attention for visual question answer-
- 1067 ing. In *European Conference on Computer Vision*, pages
- 1068 451–466. Springer, 2016. 2
- 1069
- 1070 [31] C. Zhu, Y. Zhao, S. Huang, K. Tu, and Y. Ma. Structured
- 1071 attentions for visual question answering. In *Proc. IEEE Int.*
- 1072 *Conf. Comp. Vis.*, volume 3, 2017. 2
- 1073
- 1074 [32] Y. Zhu, O. Groth, M. Bernstein, and L. Fei-Fei. Visual7w:
- 1075 Grounded question answering in images. In *Proceedings*
- 1076 *of the IEEE Conference on Computer Vision and Pattern*
- 1077 *Recognition*, pages 4995–5004, 2016. 2
- 1078
- 1079 [33] Y. Zhu, R. Mottaghi, E. Kolve, J. J. Lim, A. Gupta, L. Fei-
- 1080 Fei, and A. Farhadi. Target-driven Visual Navigation in
- 1081 Indoor Scenes using Deep Reinforcement Learning. In *IEEE International Conference on Robotics and Automation*,
- 1082 2017. 2